ADA114673

# Automatic Detectors for Frequency-Agile Radars

G. V. TRUNK

*Radar Analysis Branch*
*Radar Division*

April 23, 1982

1 9 1982

NAVAL RESEARCH LABORATORY
Washington, D.C.

| REPORT DOCUMENTATION PAGE | | READ INSTRUCTIONS<br>BEFORE COMPLETING FORM |
|---|---|---|
| 1. REPORT NUMBER<br><br>NRL Report 8571 | 2. GOVT ACCESSION NO. | 3. RECIPIENT'S CATALOG NUMBER |
| 4. TITLE (and Subtitle)<br><br>AUTOMATIC DETECTORS FOR FREQUENCY-AGILE<br>RADARS | | 5. TYPE OF REPORT & PERIOD COVERED<br>Interim report on one phase of<br>an NRL problem. |
| | | 6. PERFORMING ORG. REPORT NUMBER |
| 7. AUTHOR(s)<br><br>G. V. Trunk | | 8. CONTRACT OR GRANT NUMBER(s) |
| 9. PERFORMING ORGANIZATION NAME AND ADDRESS<br><br>Naval Research Laboratory<br>Washington, DC 20375 | | 10. PROGRAM ELEMENT, PROJECT, TASK<br>AREA & WORK UNIT NUMBERS<br>61153N; RR021-05-43;<br>NRL Problem 53-0626-0 |
| 11. CONTROLLING OFFICE NAME AND ADDRESS<br>Department of the Navy<br>Office of Naval Research<br>Arlington, VA 22217 | | 12. REPORT DATE<br>April 23, 1982 |
| | | 13. NUMBER OF PAGES<br>15 |
| 14. MONITORING AGENCY NAME & ADDRESS(If different from Controlling Office) | | 15. SECURITY CLASS. (of this report)<br><br>UNCLASSIFIED |
| | | 15a. DECLASSIFICATION/DOWNGRADING<br>SCHEDULE |

16. DISTRIBUTION STATEMENT (of this Report)

Approved for public release; distribution unlimited.

17. DISTRIBUTION STATEMENT (of the abstract entered in Block 20, if different from Report)

18. SUPPLEMENTARY NOTES

19. KEY WORDS (Continue on reverse side if necessary and identify by block number)

Detection
Square-law detector
Sidelobe jamming
Frequency diversity

20. ABSTRACT (Continue on reverse side if necessary and identify by block number)

   When frequency agility is used in radars, the received sidelobe jamming power can vary by as much as 20 dB even though the transmitted jamming power is constant over the radar bandwidth. Various detectors were compared using simulation techniques; the best detector was the ratio detector, which normalizes the received power on every pulse with the surrounding reference cells and then sums these normalized power ratios. In the presence of short-pulse interference, a low false-alarm rate can be maintained by soft-limiting of the individual power ratios.

DD FORM 1473 EDITION OF 1 NOV 65 IS OBSOLETE
1 JAN 73
S/N 0102-014-6601

# CONTENTS

iii

# AUTOMATIC DETECTORS FOR FREQUENCY-AGILE RADARS

## INTRODUCTION

Modern, long-range surveillance radars can detect 1-m$^2$ targets at ranges of 200 nmi or longer. However, if the radar transmits at a constant frequency, a jammer needs only to jam a narrow bandwidth to reduce significantly the radar detection range. To force the jammer to do broadband jamming, and consequently to reduce its effectiveness, most modern radars employ pulse-to-pulse frequency agility. When frequency agility is used, the received sidelobe jamming power can vary by as much as 20 dB pulse-to-pulse even though the transmitted jamming power is constant over the radar bandwidth. To see why this is true, consider Fig. 1, which shows the measured jamming power received by the SPS-39 radar as it scans by a jammer [1]. In a space of several degrees the jamming power usually varies by 15 dB and sometimes varies by 20 or more dB. These data were recorded at a constant frequency. Thus, if the frequency is varied pulse-to-pulse, the sidelobes pointed in the direction of the jammer will shift by several degrees; therefore the received sidelobe jamming power will vary pulse-to-pulse by as much as 20 dB.
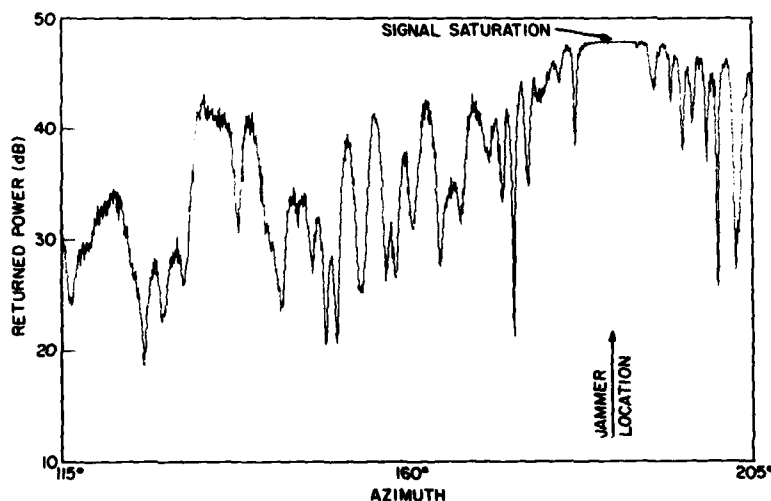


Fig. 1 — Received jamming power as the SPS-39 radar sweeps over a jammer

The present automatic detectors planned and deployed in the fleet do *not* take advantage of the fact that the received jamming power varies when frequency agility is employed. The purpose of this report is to investigate the detection performance of various detectors for a radar employing frequency agility in the presence of broadband sidelobe jamming.

## AUTOMATIC DETECTORS

If the jamming is white Gaussian noise, the density of the $i$ th output pulse $x_i$ from an envelope detector is

$$p(x_i|A_i) = \frac{x_i}{\sigma_i^2} \exp[-(x_i^2 + A_i^2)/2\sigma_i^2]I_0(A_i x_i/\sigma_i^2), \tag{1}$$

where $A_i$ is the signal amplitude, the signal-to-noise ratio $(S/N)$ is $10 \log(A_i^2/2\sigma_i^2)$, and the noise power $\sigma_i^2$ varies pulse-to-pulse because frequency agility is being used in the presence of sidelobe jamming. The detection problem of interest is

$$H_0: \ A_i \equiv 0, \ \text{any} \ \sigma_i;$$

$$H_1: \ A_i > 0, \ \text{any} \ \sigma_i.$$

Since $\sigma_i$ is unknown, no uniformly most powerful test exists. That is, no optimal (in the sense of maximizing the probability of detection for a given false-alarm probability) test exists, and suboptimal tests must be used.

We proceed by first assuming that $\sigma_i$ and $A_i$ are known. Then the optimal test statistic is the likelihood ratio

$$L = \prod_{i=1}^{n} [p(x_i|A_i)/p(x_i|A_i = 0)], \tag{2}$$

where $x_1, \ldots, x_n$ are $n$ independent samples. A target is declared when $L$ is greater than the threshold which determines the probability of false alarm $(P_{fa})$. Using a small-signal approximation, we can show that the likelihood test is equivalent to comparing

$$\sum_{i=1}^{n} A_i^2 x_i^2/\sigma_i^4 \tag{3}$$

to an appropriate threshold. Unfortunately, in the problem of interest $A_i$ and $\sigma_i$ are unknown. To proceed, we will set $A_i = 1$ and use neighboring samples to estimate $\sigma_i$. Thus, the new test statistic is

$$\sum_{i=1}^{m} \frac{x_i^2}{\hat{\sigma}_i^2},$$

which is implemented by

$$\sum_{i=1}^{n} \frac{x_i^2(j)}{\frac{1}{2m} \sum_{k=1}^{m} [x_i^2(j + 1 + k) + x_i^2(j - 1 - k)]}, \tag{4}$$

where $x_i(j)$ is the $i$ th envelope-detected pulse in the $j$ th range cell and $2m$ is the number of reference cells. The denominator is the maximum likelihood estimate of $\sigma_i^2$ and, essentially, the detector sums signal-to-noise power ratios. This detector, which we will call the ratio detector, is shown in Fig. 2.

The ratio detector has good performance because it sums power ratios. Thus, it will detect targets even though only a few returned pulses have a high signal-to-noise ratio. Unfortunately, this will also cause the ratio detector to declare false alarms in the presence of short-pulse interference.* Consequently, to reduce the number of false alarms when short-pulse interference is present, the individual

---

*In radars which use pulse compression, any short-pulse interference will be spread out to the transmitted-pulse width and, therefore, the ratio detector can be used without introducing a large number of false alarms. Of course, if radars are using similar pulse-compression networks (e.g., linear FM), long interference pulses will be compressed into interference spikes.
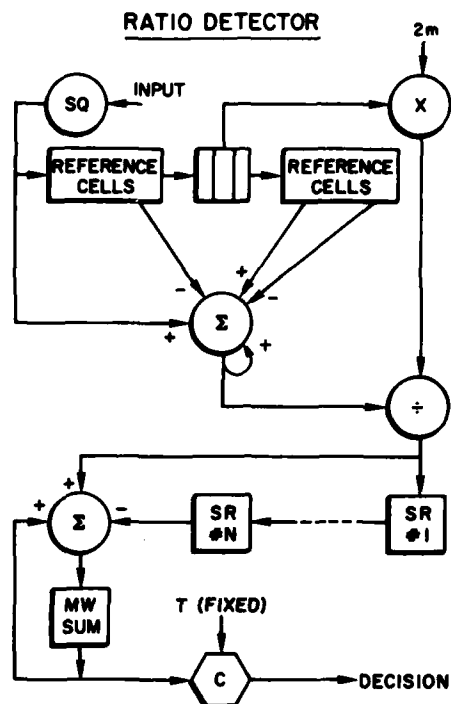
RATIO DETECTOR

Fig. 2 — Ratio detector: SR is a shift register, MW is a moving window, 2m is the number of reference cells, and C is a comparator

power ratios will be soft-limited to a small enough value so that interference will only cause a small number of false alarms.

In some cases, limiting will have very little effect on the detection performance of the ratio detector. In a previous study [1] signals were numerically injected into the recorded data shown in Fig. 1, and a comparison was made between the ratio detector and the cell-averaging CFAR. The original detection results are shown in Fig. 3. At each azimuth beam position there were 12 detection opportunities. Of the two detectors, the ratio detector has better performance when the jamming power changes rapidly with aspect angle. This comparison was repeated with the individual ratios being limited to a value of 12. Comparing the new results in Fig. 4 with the old results in Fig. 3, one notes that the detection performance of the ratio detector with or without limiting is practically the same. However, since we know nothing about the optimal detection properties of the soft-limiting ratio detector, we will compare its detection performance with the more commonly used detectors, such as the cell-averaging CFAR, the log integrator, and the binary integrator. These detectors can be described mathematically as follows: The cell-averaging CFAR is given by

$$\frac{\sum_{i=1}^{n} x_i^2(j)}{\frac{1}{2m} \sum_{k=1}^{m} \sum_{i=1}^{n} [x_i^2(j+1+k) + x_i^2(j-1-k)]} ; \tag{5}$$

and the log integrator is given by

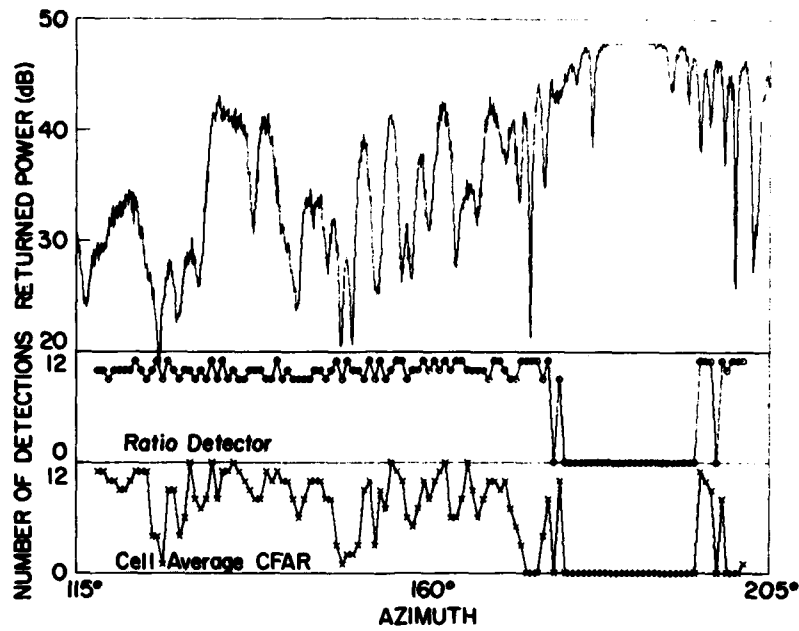$$\sum_{i=1}^{n} [\log x_i(j) - \overline{\log x_i(j)}], \tag{6}$$

Fig. 3 — Comparison of ratio detector (no limiting) and cell-averaging CFAR
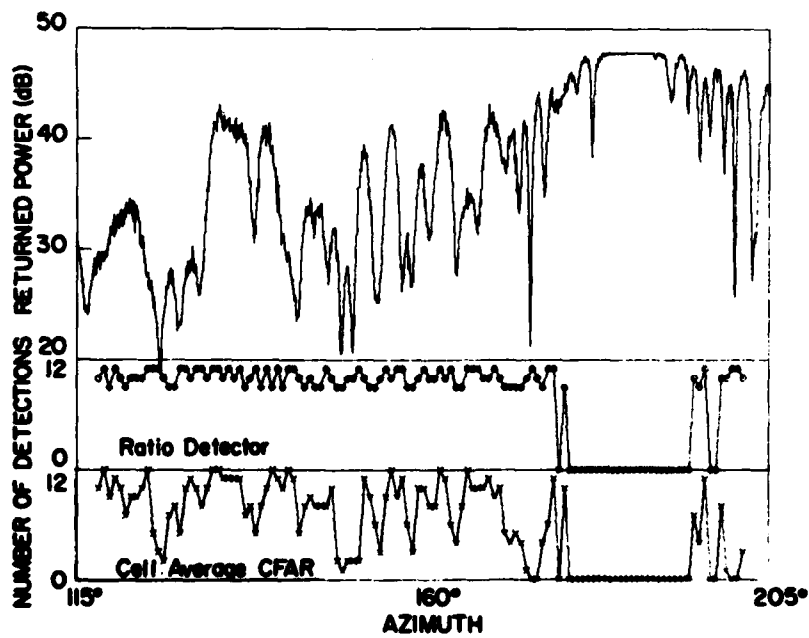using recorded sidelobe jamming data



Fig. 4 — Comparison of ratio detector (limiting) and cell-averaging CFAR
using recorded sidelobe jamming data

4

where

$$\overline{\log x_i(j)} = \frac{1}{2m} \sum_{k=1}^{m} [\log x_i(j + 1 + k) + \log x_i(j - 1 - k)];$$ (7)

and the binary integrator is given by

$$\sum_{i=1}^{n} y_i(j),$$ (8)

where

$$y_i(j) = \begin{cases} 0 \text{ if } [\log x_i(j) - \overline{\log x_i(j)}] < T, \\ 1 \text{ if } [\log x_i(j) - \overline{\log x_i(j)}] \geqslant T. \end{cases}$$ (9)

We will compare these detectors by first calculating the appropriate detection thresholds using the importance-sampling technique and then calculating the detection performance using a straightforward Monte Carlo simulation.

## DETECTION THRESHOLDS

As noted previously [1], the ratio detector is the sum of samples from an F-distribution, and its density function can only be represented in terms of an integral. To avoid numerical integrations, the detection threshold will be calculated using the importance-sampling technique [1-3]. Since many simulations were run, we chose to use only $n = 6$ pulses integrated and $2m = 16$ reference cells. These numbers correspond to those of the NRL radar which will eventually be used to record data to validate the simulation results. The results for the ratio detector are shown in Fig. 5.

As mentioned previously, if short-pulse interference is present, the ratio detector will have too many false alarms. To relieve this problem the individual ratio was limited to a maximum value of 10, the simulation was repeated, and the results are shown in Fig. 6.

To show that limiting will yield a low false-alarm rate in the presence of nonsychronous interference, we will calculate the false-alarm rate when the probability of an interference spike is $10^{-3}$ in each range cell. The probability of false alarm is

$$P_{FA} = \sum_{i=0}^{n} P_{FA}(i)P(i),$$ (10)

where $P_{FA}(i)$ is the conditional probability of false alarm given that $i$ interference spikes are present in the $n$ pulses, $P(i)$ is the probability that there are exactly $i$ interference spikes present, and $P(i)$ is binominally distributed. The detection threshold is set so that $P_{FA} = 10^{-6}$ if there are no spikes present. Thus, from Fig. 6, the threshold is set equal to 29.2. The calculation of $P_{FA}$ proceeds as follows: for $i = 0$ (i.e., no spikes present) $P(0) = 0.994$ and $P_{FA}(0) = 10^{-6}$. For $i = 1$ (one spike present), $P(1) = 0.006$, and $P_{FA}(1)$ equals the probability that the sum of the other five ratios exceeds 19.2 (here we are assuming that the ratio containing the spike obtains the limiting value; hence 29.2 − 10.0 = 19.2). From Fig. 6, $P_{FA}(1) = 2.0 \times 10^{-4}$. Similarly, for $i = 2$, $P(2) = 15 \times 10^{-6}$ and $P_{FA}(2) = 0.036$. Since $P(3) = 20 \times 10^{-9}$, the probabilities associated with $i = 3, 4, 5,$ and 6 can be neglected. Substituting the previously calculated probabilities into Eq. (10) yields $P_{FA} = 2.7 \times 10^{-6}$. Thus, limiting can be used to obtain a low false-alarm rate when short-pulse interference is present. The limiting value of 10 was found by trying various values. For instance, if the limiting value is 12, $P_{FA} = 6.5 \times 10^{-6}$.
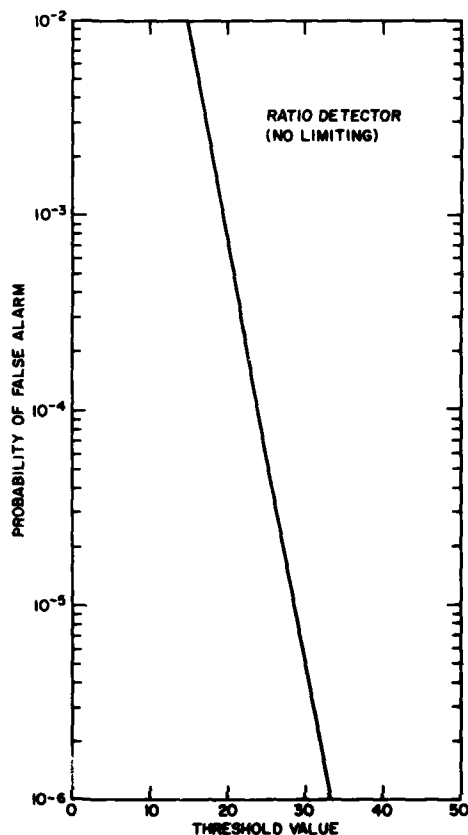
5

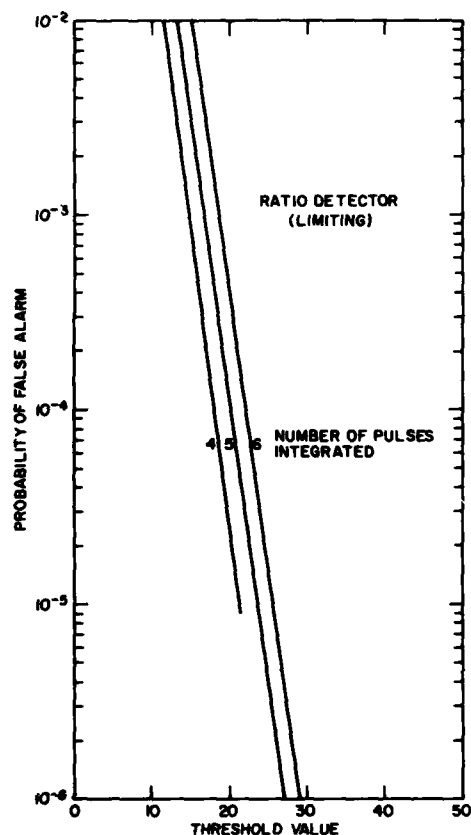Fig. 5 — Threshold values for the ratio detector: six pulses integrated and 16 reference cells used

Fig. 6 — Threshold values for the ratio detector: four, five, or six pulses integrated; 16 reference cells used; maximum value of each ratio limited to a value of 10

The importance-sampling technique was used to calculate the thresholds for the cell-averaging CFAR, the log integrator, the log integrator with a limiting value of 1.5, and the single-pulse log detector which is needed for the binary integrator. The threshold curves are given in Figs. 7 to 10. Using Fig. 9, the $P_{FA}$ in the presence of interference is calculated to be $1.7 \times 10^{-6}$ when the log integrator is limited to a value of 1.5. Using Fig. 10, the appropriate thresholds yielding $P_{FA}(0) = 10^{-6}$ for 2 out of 6, 3 out of 6, and 4 out of 6 detectors are found to be 1.51, 1.27, and 1.10, respectively.

## DETECTION RESULTS

To compare the performance of the various detectors, probability-of-detection vs signal-to-noise-ratio curves were generated using simulation techniques. Results are for the case of six pulses integrated, 16 reference cells, and a false-alarm probability of $10^{-6}$ in thermal noise. The detection performance for nonfluctuating and pulse-to-pulse Rayleigh fluctuating targets in thermal noise (i.e., no jamming) of the five detectors discussed is shown in Figs. 11 and 12, respectively. For nonfluctuating targets, the cell-averaging CFAR is the best detector; however, the ratio detector and log integrator are within a few tenths of a decibel. The binary integrator is 1 to 1.5 dB worse than the cell-averaging CFAR. On the other hand, for Rayleigh fluctuations, the variation is between 0 and 3 dB. The cell-averaging CFAR is still the best detector. The ratio detector is better than the log integrator, which is better than the binary integrator.
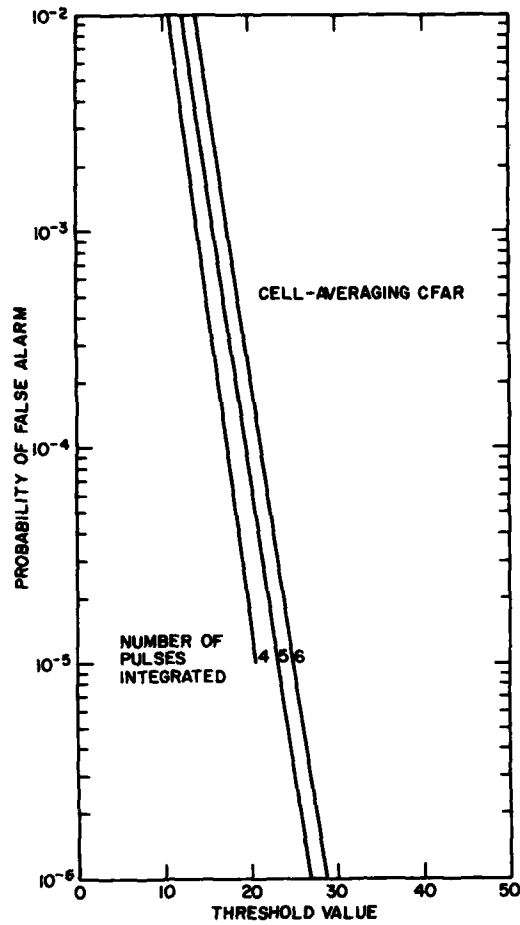
6

Fig. 7 — Threshold values for the cell-averaging
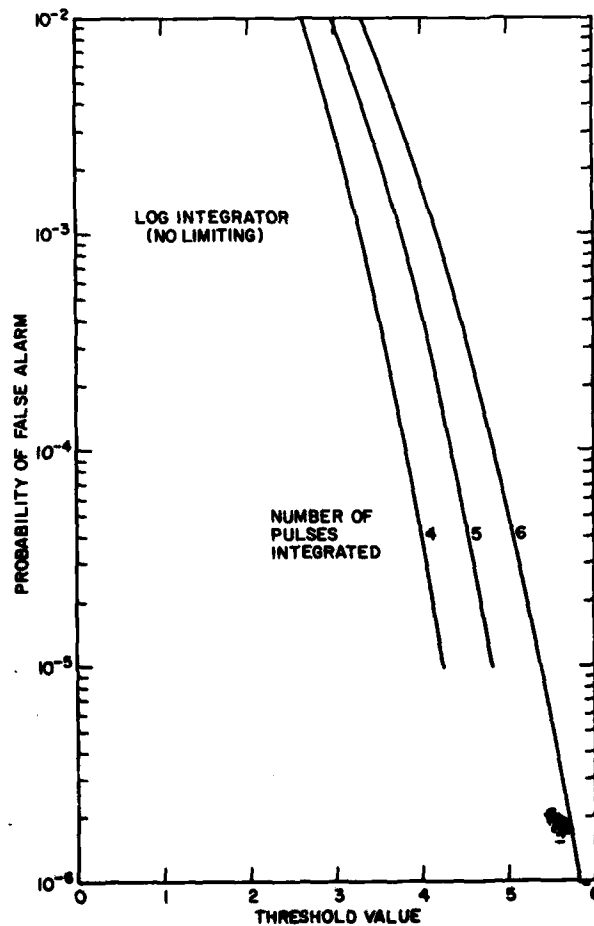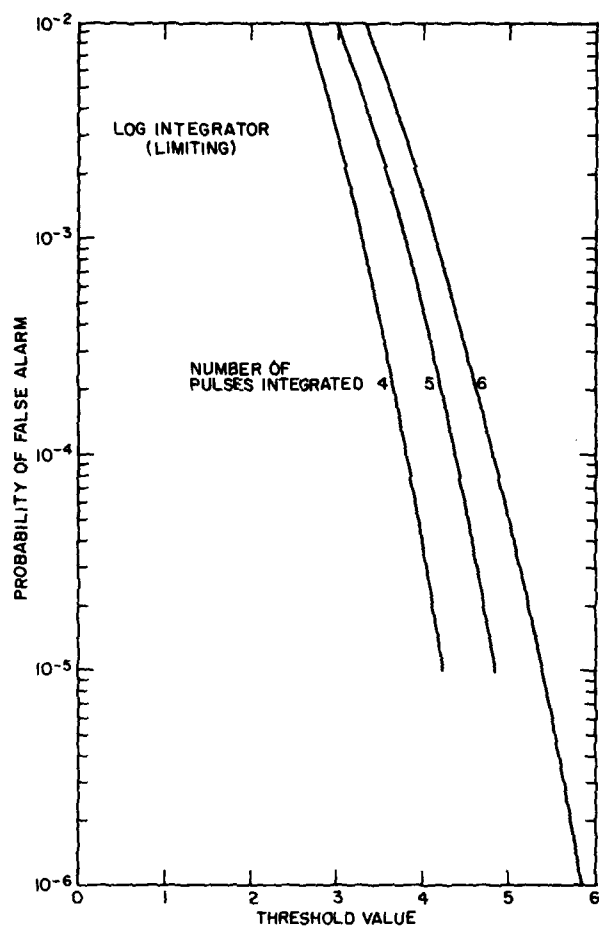CFAR: four, five, or six pulses integrated and 16
reference cells used

CELL-AVERAGING CFAR

NUMBER OF
PULSES
INTEGRATED

4 5 6

PROBABILITY OF FALSE ALARM

THRESHOLD VALUE

LOG INTEGRATOR
(NO LIMITING)

NUMBER OF
PULSES
INTEGRATED

4 5 6

PROBABILITY OF FALSE ALARM

THRESHOLD VALUE

Fig. 8 — Threshold values for the log integrator: four, five,
or six pulses integrated and 16 reference cells used

7

Fig. 9 — Threshold values for the log integrator: four, five, or six pulses integrated; 16 reference cells used; and maximum value of each normalized log term limited to a value of 1.5
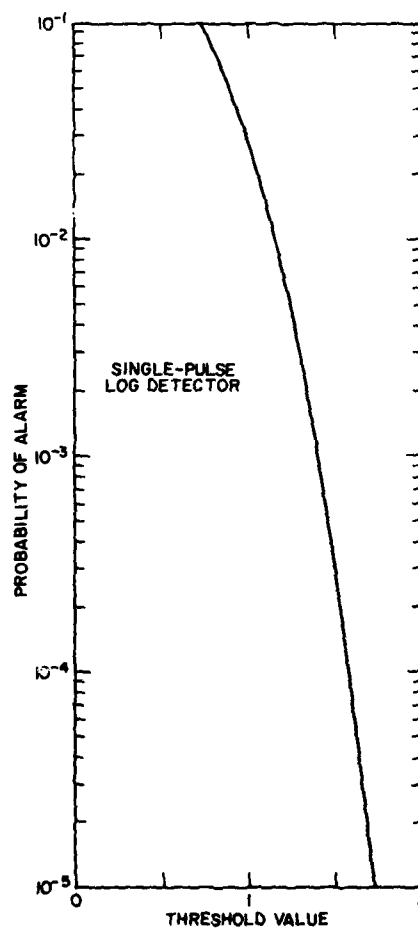


Fig. 10 — Threshold values for single-pulse log detector: 16 reference cells used
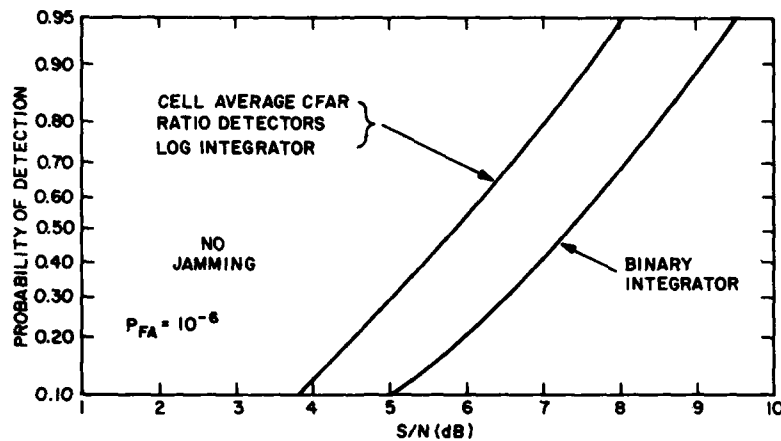
Fig. 11 — Curves of probability of detection vs signal-to-noise ratio for the cell-averaging CFAR, ratio detectors, log integrator, and binary integrator: nonfluctuating target and probability of false alarm $= 10^{-6}$
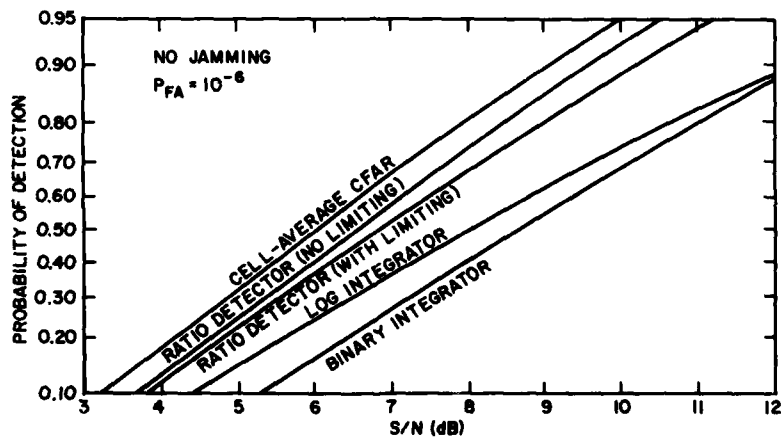


Fig. 12 — Curves of probability of detection vs signal-to-noise ratio for the cell-averaging CFAR, ratio detectors, log integrator, and binary integrator: Rayleigh fluctuating target and probability of false alarm $= 10^{-6}$

To compare the various detectors in jamming it was first necessary to generate the variation of jamming power when frequency agility is employed. The received jamming power can be written as

$$J = C\,G^2,$$

where $C$ is an appropriate constant (a function of jammer power, jammer antenna gain, and range from jammer to radar) and $G$ is the radar-antenna voltage gain in the direction of the jammer. In the far-out sidelobe region, it is a reasonable assumption that the gain varies as $(\sin x)/x$.* Therefore, when one

---

*The sidelobe antenna pattern varies as $(\sin x)/x$ if the antenna aperture has a uniform distribution across it. However, aboard a naval ship the sidelobe antenna pattern is determined by the ship's superstructure located close to the antenna. Therefore, the sidelobe antenna pattern is usually extremely complicated, as is indicated in Fig. 1. However, since there does not exist any good model for realistic sidelobe antenna patterns, we will use the simple $(\sin x)/x$ model.

9

changes the radar frequency, the variable $x$, which is proportional to frequency, changes and consequently the received jamming power changes. If one assumes that $x$ is uniformly distributed from $x_0$ to $x_0 + 2\pi$ (where $x_0$ is any angle for which $|x_0| \geqslant \pi$), then the jamming $J$ is approximately proportional to $\sin^2 x$, and the probability density of $J$ (normalized to a maximum value of 1) is given by

$$P(J) = \frac{1}{(J - J^2)^{1/2}}, \quad 0 \leqslant J \leqslant 1. \tag{11}$$

This density is plotted in Fig. 13. Thus, the total noise-plus-jamming power is given by

$$\sigma^2 = 1 + J_0^2 J, \tag{12}$$

where $J_0^2$ is the maximum received jamming power, $J$ is a random variable between 0 and 1 whose density is given by Eq. (11), and the thermal noise power has been set to 1. The signal-to-noise ratio is defined as

$$S/N\,(\mathrm{dB}) = 10 \log (A^2/2), \tag{13}$$

where $A$ is the nonfluctuating signal amplitude, and the maximum jamming-to-noise ratio is given by
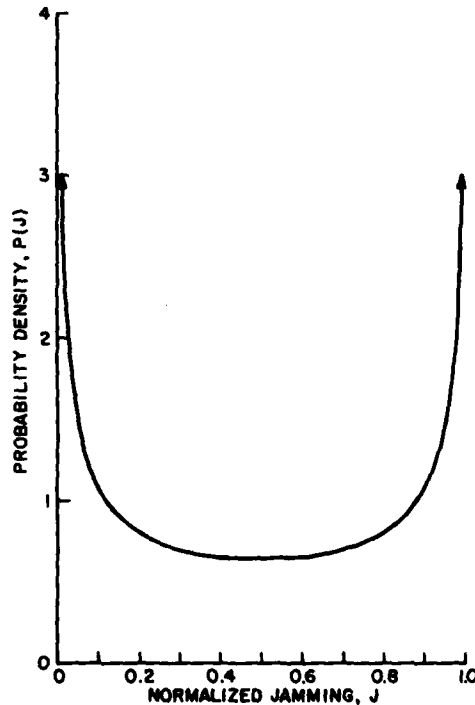
$$J/N\,(\mathrm{dB}) = 10 \log (J_0^2). \tag{14}$$



Fig. 13 — Normalized probability density of jamming power

Detection curves for nonfluctuating targets in jamming are shown in Figs. 14 and 15. Now the ratio detector is better than the log integrator, which is better than the cell-averaging CFAR, which is better than the binary integrator. When $J/N = 10$ dB, the detectors differ by 2 dB; however, when $J/N = 20$ dB, the detectors differ by as much as 8 dB.
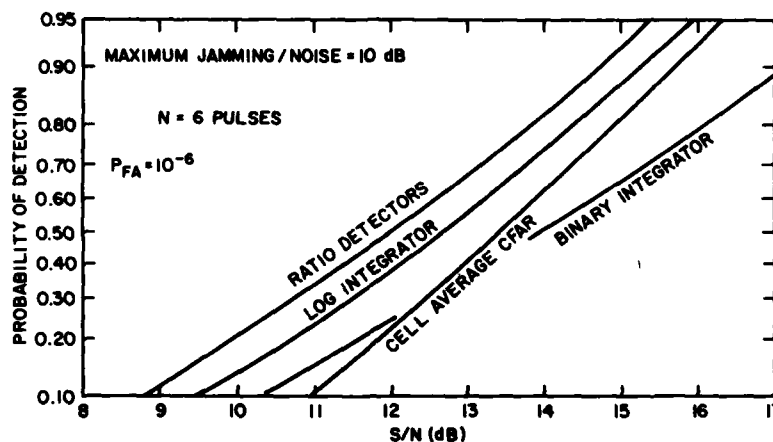
10

Fig. 14 — Curves of probability of detection vs signal-to-noise ratio for the cell-averaging CFAR, ratio detectors, log integrator, and binary integrator: nonfluctuating target, probability of false alarm = $10^{-6}$, and maximum jamming-to-noise ratio = 10 dB
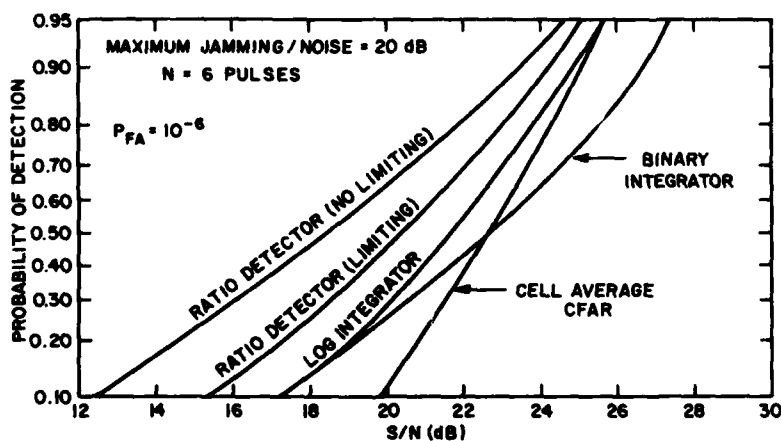


Fig. 15 — Curves of probability of detection vs signal-to-noise ratio for the cell-averaging CFAR, ratio detectors, log integrator, and binary integrator: nonfluctuating target, probability of false alarm = $10^{-6}$, and maximum jamming-to-noise ratio = 20 dB

The results for Rayleigh fluctuating targets are shown in Figs. 16 and 17. The ratio detector is still the best detector. However, the next-best detector is the cell-averaging CFAR. The log integrator and binary integrator are very similar in performance.

All of the previous results for the jamming cases were based on the assumption that the jamming power varied as $[(\sin x)/x]^2$. To test the sensitivity of the results to this assumption, the Rayleigh fluctuating case where $J/N = 20$ dB was repeated, assuming that the jamming power was uniformly distributed. The results for this case are shown in Fig. 18. While Figs. 17 and 18 are different, the same relationship is maintained between the detectors.
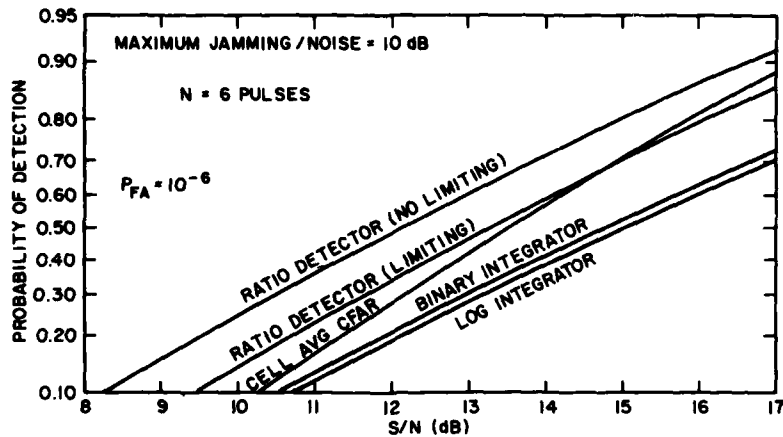
11

Fig. 16 — Curves of probability of detection vs signal-to-noise ratio for the cell-averaging CFAR, ratio detectors, log integrator, and binary integrator: Rayleigh fluctuations, probability of false alarm = $10^{-6}$, and maximum jamming-to-noise ratio = 10 dB
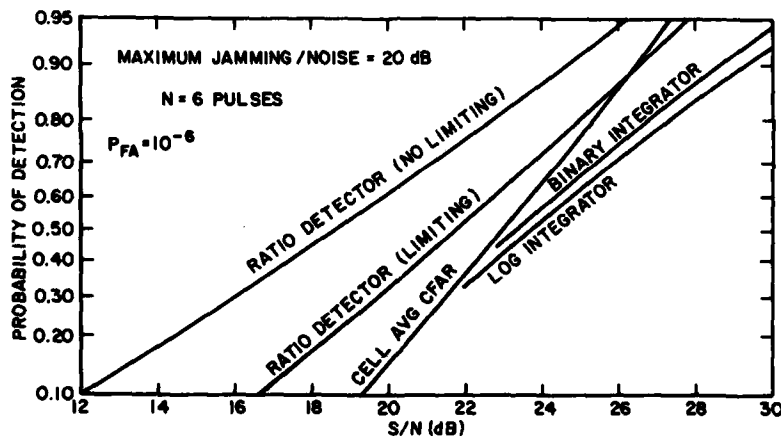


Fig. 17 — Curves of probability of detection vs signal-to-noise ratio for the cell-averaging CFAR, ratio detectors, log integrator, and binary integrator: Rayleigh fluctuations, probability of false alarm = $10^{-6}$, and maximum jamming-to-noise ratio = 20 dB

In the jamming cases considered, the ratio detector without limiting was the best detector and the ratio detector with limiting was the next-best detector. In thermal noise, the ratio detectors are only several tenths of a dB worse than the cell-averaging CFAR. Therefore, if one does not have any short-pulse interference problems, one should use the ratio detector; and if one does have short-pulse interference problems, one should use the ratio detector with limiting. Since the ratio detector without limiting can be several dB better than the ratio detector with limiting, one possibility is to use the ratio detector without limiting and then perform a second test using the individual ratios (i.e., not the sum) to test whether the received signal is from a target or is interference. We are presently investigating this technique but are having difficulty in generating a suitable test.
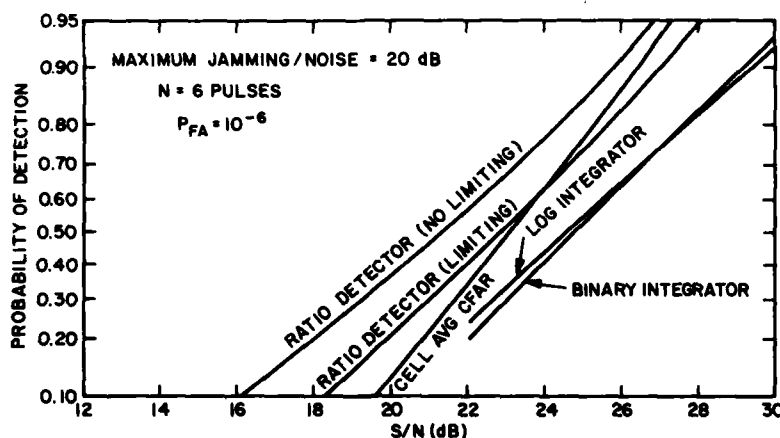
Fig. 18 — Curves of probability of detection vs signal-to-noise ratio for the cell-averaging CFAR, ratio detectors, log integrator, and binary integrator: Rayleigh fluctuations, probability of false alarm = $10^{-6}$, maximum jamming-to-noise ratio = 20 dB, and jamming power is uniformly distributed

Some people would note that the ratio detectors are very susceptible to target suppression and, therefore, should not be used. However, when pulse-to-pulse frequency agility is used, coherent cancellation techniques for clutter cannot be used and one then requires a very suppressing type of detector to avoid false alarms in clutter.

## SUMMARY

When pulse-to-pulse frequency agility is employed, the received sidelobe jamming power can vary by as much as 20 dB. The best detector for this situation is the ratio detector, which normalizes the received *power* on every pulse (using the neighboring reference cells) and then sums these normalized power ratios. In the presence of short-pulse interference, a ratio detector using limiting should be employed.

There are two areas which require further work. First, pulse-to-pulse frequency agility should be used in the presence of broadband sidelobe jamming, and the recorded data should be used to test the behavior of the various detectors mentioned in this report. Second, one should continue investigating whether the ratio detector without limiting can be used in the presence of short-pulse interference by performing a second test to discriminate between target and interference using the individual ratios, not the sum.

## REFERENCES

1. G.V. Trunk, "Comparison of Detectors in the Presence of Sidelobe Jamming," NRL Report 8449, Oct. 23, 1980.

2. V.G. Hansen, "Importance Sampling in Computer Simulation of Signal Processors," Comput. Electr. Eng. 1, 545-550 (1974).

3. R.L. Mitchell, "Importance-Sampling Applied to Simulation of False Alarm Statistics," IEEE Trans. Aerosp. Electron. Syst. AES 17(1), 17-24 (Jan. 1981).